Babylonian Journal of Networking
Vol.2024, **pp**. 122–134
DOI: https://doi.org/10.58496/BJN/2024/013; ISSN: 3006-5372
https://mesopotamian.press/journals/index.php/BJN

Research Article

# Performance Analysis of Hybrid Optical OFDM Schemes in terms of PAPR, BER and Spectral Efficiency using Various PAPR Reduction Methods

Karthik Kumar Vaigandla [1,*], Mounika Siluveru [1], Dharavath Nanda [1], Radhakrishna Karne [2]

[1] *Electronics and Communications Engineering, Balaji Institute of Technology and Science, Telangana, India.*

[2] *Electronics and Communications Engineering, CMR Institute of Technology, Hyderabad, Telangana, India.*

**ARTICLE INFO**

Article History

Received 20 May 2024
Revised 30 Jun 2024
Accepted 19 Jul 2024
Published 01 Aug 2024

Keywords

ACO-OFDM
ADO-OFDM
BER
DCO-OFDM
Optical
OFDM
PAPR
SLM
LACO-OFDM

**ABSTRACT**

Orthogonal Frequency Division Multiplexing (OFDM) is an extremely important technique for transmitting data in both optical wireless and optical fiber communication. Optical wireless systems are limited to transmitting real and positive values to the optical transmitter, since they rely only on the intensity of a signal to convey information. Consequently, traditional OFDM is not suitable for direct implementation in optical systems. Various altered OFDM schemes have been examined to counteract multipath distortion, such as DC-biased optical OFDM (DCO-OFDM), asymmetrically clipped optical OFDM (ACO-OFDM), asymmetrically clipped DC biased optical OFDM (ADO-OFDM) and layered asymmetrically-clipped optical OFDM (LACO-OFDM) technique to improve the bit error rate (BER) performance and spectral efficiency of optical system. This article explores ways for reducing Peak-to-Average Power Ratio (PAPR). A mathematical model is formulated to account for clipping and Selective Mapping (SLM), as well as channel noise, in all of these approaches for received signal. LACO-OFDM has been determined to be a superior option when compared to other techniques. LACO-OFDM, a recently developed technique, demonstrates excellent performance in terms of PAPR, BER, and spectral efficiency. The simulation results demonstrate that the LACO-OFDM approach has greatly enhanced the spectral efficiency in comparison to previous approaches.

## 1. INTRODUCTION

OFDM is commonly employed in wired and wireless broadband communication systems because it efficiently reduces inter-symbol interference (ISI) caused by a dispersed channel. OFDM has the added advantage of requiring a simple single-tap equaliser at the receiver. OFDM is gaining prominence as a modulation technique for optical systems. It has higher optical power efficiency than standard modulation systems such as OOK and PPM. Traditional OFDM sends bipolar and complex signals [1-2]. However, bipolar signals cannot be sent in an intensity modulated/direct detection (IM/DD) optical wireless system because light intensity cannot be negative. OFDM signals designed for IM/DD systems must be real and non-negative. Other types of OFDM utilized in IM/DD systems include ACO-OFDM, DCO-OFDM, and variants based on ACO-OFDM and DCO-OFDM.

In ACO-OFDM, the transmitted signal is corrected by truncating the original bipolar OFDM signal at zero and broadcasting just the positive components. DCO-OFDM employs a DC bias to keep the signal positive. In ACO-OFDM, only subcarriers with odd indices are utilised to transmit data. In contrast, DCO-OFDM transports data symbols across all subcarriers. ACO-OFDM surpasses DCO-OFDM in terms of average optical power for quadrature amplitude modulation (QAM) constellations such as 4-QAM, 16-QAM, 64-QAM, and 256-QAM. However, when dealing with larger constellations, such as 1024 QAM and 4096 QAM, DCO-OFDM outperforms. The inefficiency of optical power in DCO-OFDM is caused by the use of DC bias, while the inefficiency of bandwidth in ACO-OFDM is caused by the use of just half of the subcarriers. For smaller constellations, the main effect is greater, and ACO-OFDM outperforms other technologies. However, for larger constellations, the secondary impact becomes more apparent, and DCO-OFDM performs better.

*Corresponding author. Email: vkvaigandla@gmail.com

OFDM is a standard RF wireless communication technology. Due to RF-based OFDM's limited transmission speeds, data, audio, and video services are growing, necessitating alternate methods. The concept recommends IM/DD-based O-OFDM to boost data rates [3]. Since intensity cannot be negative, O-OFDM transmits only positive signals, unlike typical RF OFDM. In IM/DD-based optical OFDM, the transmitted signal is genuine and positive. DCO, ACO, and ADO optical OFDM are the primary kinds. DCO-OFDM was one of the first IM/DD unipolar signal generators [4]. DC biasing in DCO-OFDM aims to unipolarize bipolar signals. Bipolar OFDM signals have a minimum amplitude equal to the DC bias needed to transform them to unipolar. Therefore, biasing increases DCO-OFDM power needs dramatically. To reduce power usage, ACO-OFDM is recommended [5-6]. No direct current bias is needed to create a unipolar signal [7]. DCO-OFDM transports data using even and odd subcarriers, while ACO-OFDM uses just odd. ACO-OFDM has a lower data transmission rate than DCO-OFDM [8].

## 2. SYSTEM MODEL

### 2.1 Conventional OFDM model

Several digital modulation methods, such as PSK, QPSK, and QAM, have been developed to facilitate the modulation of binary input sequences. The modulated symbols were partitioned into frames of OFDM, each having a length of N. The OFDM signal represents the combination of N separate subcarriers, each with the same bandwidth [9-11]. This may be stated as:

$$X = \left[x_0, x_1, ...., x_{N-1}\right]^T \tag{1}$$

The serial-to-parallel (S/P) converter is responsible for transferring the frames to the Inverse Fast Fourier Transform (*IFFT*) and OFDM baseband. This conversion occurs after the modulated symbols $X_k$ have passed through an IFFT block. Subsequently, the nth sample of the N OFDM signal used for transmitting discrete-time data is represented as:

$$x_n = x(n) = \frac{1}{\sqrt{N}} \sum_{k=0}^{N-1} X(k) e^{\frac{j2km\pi}{N}} \tag{2}$$

The PAPR of OFDM signals exhibits more variability due to the addition of subcarriers with identical phases, resulting in an increase in signal peaks with higher power levels. Regarding the OFDM-based visible-light-communication (VLC) schemes, it was shown that the LEDs were the primary source of nonlinearity [12]. This is because the maximum signal amplitude was restricted by the dynamic range of the LEDs. Simply said, the PAPR is a measure of the ratio between the highest peak power and the average power. This concept is further explained below:

$$PAPR_{db} = \frac{P_{peak}}{P_{average}} = \frac{Max\left|x_n\right|^2}{E\left[\left|x_n\right|^2\right]} \tag{3}$$

Here, $x_n$ represents a discrete-time signal. The number of subcarriers is N and E[.] represents expectation. The High Power Amplifier (HPA) suffered nonlinear distortion from analogue domain, but OFDM signal processing to decrease PAPR may be done digitally. The digital PAPR differs from the analogue one. However, the analogue PAPR was approximated by oversampling the digital signal [13]. The nonlinear amplification of the Power Amplifier (PA) reduces HPA efficiency, therefore a larger PAPR or envelope volatility can significantly reduce system performance. This causes in-band signal distortion and OoB radiation. A waveform with a higher peak power is supplied in the linear section of the HPA after decreasing the input signal average power to prevent nonlinear distortion. The input back off (IBO) produced a corresponding output back-off [14]. The IBO can be presented as:

$$IoB = 10.\log_{10}\left[\frac{P_{inSat}}{P_{in}}\right] \tag{4}$$

DACs and HPAs' nonlinear properties affected OFDM signals with a greater PAPR. Previous studies have approximated PAPR values in continuous-time OFDM signals using an oversampling factor of $L \geq 4$. The Complementary Cumulative Distribution Function (CCDF) was frequently utilised to evaluate PAPR reduction procedures. The risk that the OFDM

signal PAPR will exceed PAPR0 is represented by this CCDF. A simple approximation for OFDM signals with N subcarriers' CCDF of PAPR is possible. The derivation follows:

$$CCDF = \Pr obability\left[ P\left( PAPR > PAPR_0 \right) \right] \tag{5}$$

$$CCDF = 1 - \left[ e^{-PAPR_0} \right]^{NL} \tag{6}$$

## 2.2 DCO-OFDM

A high DC bias increases optical energy per bit to single-sided noise power spectrum density. The process wastes optical power. To reduce distortion, a minor bias is utilised, and any remaining negative peaks are clipped out, causing clipping noise. In standard DCO-OFDM systems, both odd and even subcarriers carry data symbols, hence clipping noise affects all subcarriers. Negative troughs following DC bias are terminated to zero. The shortened signal enters an optical modulator. Perfect optical modulators produce a straight relation between output optical signal intensity and input electrical current. Signals are sent on flat channels [15]. The signal is subject to electrically induced shot noise, which is additive white Gaussian noise (AWGN). A photodiode converts the incoming optical signal to electrical at the receiver. Similar processing occurs as with a typical OFDM receiver. After filtering the photodiode output, the signal is digitalized. After removing the cyclic prefix (CP), the signal is converted from serial to parallel. Fast Fourier Transform inputs are signals. Following decipherment, the data is converted from parallel to serial format to preserve data signal integrity.

DCO-OFDM allows the complex data signal, denoted as , to be sent over the IFFT block. The DCO-OFDM signal exhibits Hermitian symmetry, which is defined as follows:

$$X_p = X_{N-p}^{*} \; for \; 0 < p < \frac{N}{2} \tag{7}$$

The $q^{th}$ sample of the time domain signal x, denoted as $x_q$, is provided by

$$X_q = \frac{1}{N} \sum_{p=0}^{N-1} X_p e^{\frac{j2\pi pq}{N}} \tag{8}$$

The IFFT points are represented by the symbol N, while Xq refers to the $q^{th}$ subcarrier of the signal. In order to preserve Hermitian symmetry, we establish the condition that $X_0$ is equal to $S_{N/2}$, and both are equal to zero.
The vector X may be expressed as:

$$X = X_{even} + X_{odd} \tag{9}$$

The applied DC bias is represented by the symbol $B_{DC}$. $B_{DC}$ is determined by the standard deviation of x(t).

$$B_{DC} = \rho \sqrt{E\left[ x(t)^2 \right]} \tag{10}$$

Where ρ is a constant of proportionality. If there are any remaining negative peaks after applying the DC bias, they are truncated to the zero level. Consequently, the signal that is sent will be

$$X_{DCO} = X_{even} + X_{odd} + \rho \sqrt{E\left[ x(t)^2 \right]} + N_{cBDC} \tag{11}$$

$N_{c(BDC)}$ represents the clipping noise. The clipping noise is contingent upon the direct current bias, $B_{DC}$, as previously mentioned. Eliminating negative peaks is necessary for transmitting signals without negative values. Nevertheless, the nonnegative signal obtained still exhibits significant amplitude variance, resulting in a high PAPR.

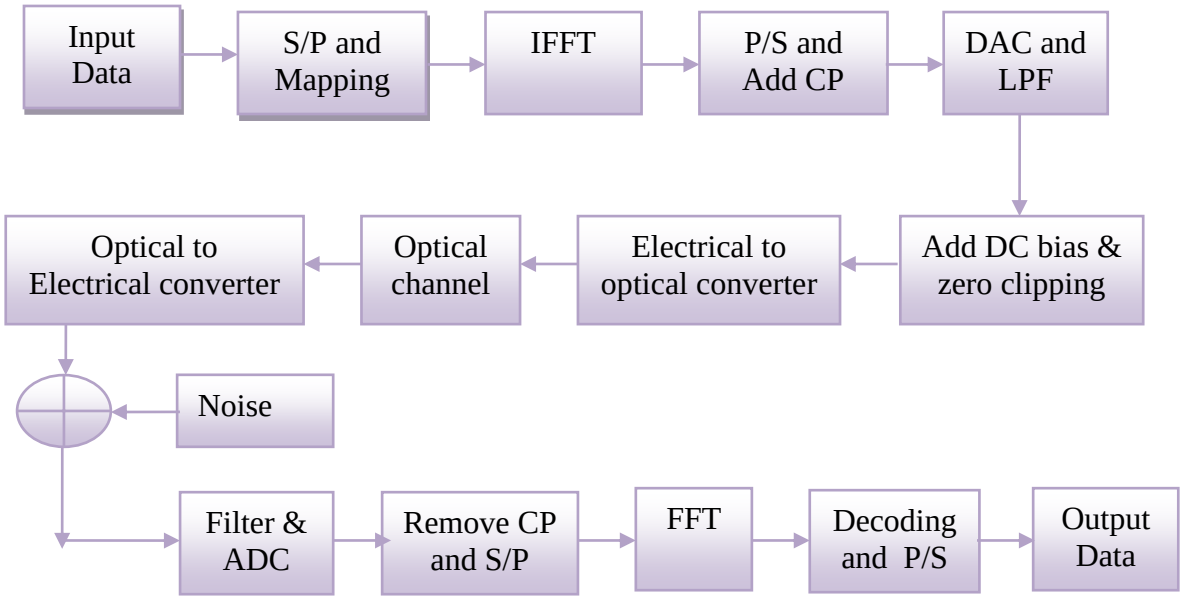


Fig. 1. DCO - OFDM

### 2.3 ACO-OFDM

The odd subcarriers carry all data symbols in ACO-OFDM, whereas the even subcarriers give a bias signal to ensure non-negativity. ACO-OFDM is shown in Figure 2. Only odd components make up the IFFT input signal. Vector components also have Hermitian symmetry. Like a DCO-OFDM transmitter, the ACO-OFDM transmitter converts data into a serialised format and adds a CP. After D/A conversion, the signal is routed through an ideal low-pass filter. Because IM/DD systems cannot transmit negative samples, the signal is truncated at zero, creating the ACO-OFDM signal. Due to signal anti-symmetry, clipping does not lose information. The ACO-OFDM signal is put into an optimum optical modulator and delivered over a flat AWGN channel. Due to their data symbols, only odd subcarriers are demodulated in ACO-OFDM, while the receiver's processing is comparable to DCO-OFDM.

The input signal X consists only of odd components, denoted as $X = [0, X_1, 0, X_3, 0, X_5 ....., 0, X_{N-1}]$, and exhibits Hermitian symmetry. The time domain signal, x, is defined as the outcome of the process.

$$x_m = -x_{m+\frac{N}{2}} \; for \; 0 < m < \frac{N}{2} \tag{12}$$

Figure 2 illustrates the several actions carried out at the transmitter. Once the signal undergoes low-pass filtering, it is referred to as x(t). By removing the negative portion of the signal, the resulting signal x(t) is transformed into the ACO-OFDM signal, $x_{ACO}(t)$. The receiver processing is the same as a DCO-OFDM receiver, except it only demodulates subcarriers with odd indices.

The requirements that are met in ACO-OFDM are as follows:

$$X(N-m) = \begin{cases} X^*(m); \; m-odd \\ 0; \; m-even \end{cases} \tag{13}$$

Let $X_c(m)$ be the $m^{th}$ frequency of the recovered ACO symbol.

$$X_c(m) = \begin{cases} \frac{X(m)}{2}; \; m-odd \\ N_c(m); \; m-even \end{cases} \tag{14}$$

In ACO-OFDM, the recovered signal value is reduced by half compared to the original value due to the transmission of data on odd subcarriers. In ACO-OFDM, the presence of noise ($N_c(m)$) is limited to the even subcarriers, resulting in received data that is free from clipping noise. The signal delivered in ACO-OFDM may be expressed as

$$X_{ACO} = \frac{X_{odd}}{2} \tag{15}$$

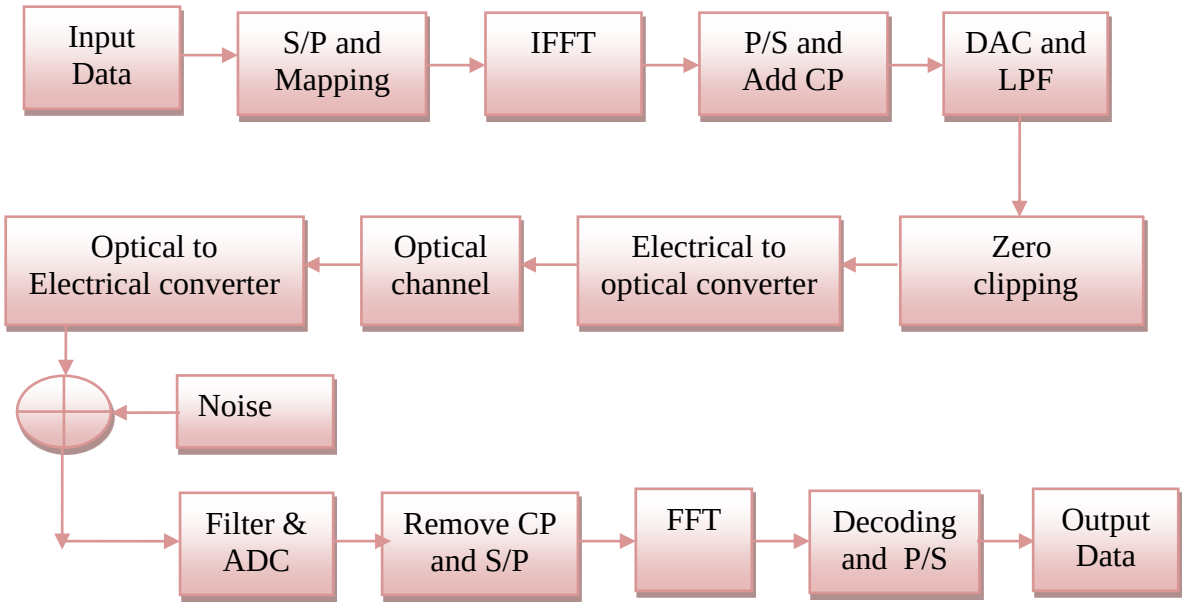


Fig. 2. ACO - OFDM

### 2.4 ADO-OFDM

This section provides a concise demonstration of the transmitter and receiver components of the standard ADO-OFDM system. The ADO-OFDM transmitter uses odd subcarriers for ACO-OFDM symbols and even subcarriers for DCOOFDM signals. By implementing the Hermitian symmetry on the modulated symbols, the frequency-domain DCO-OFDM signals may be expressed as

$$X = \left[0, 0, X2, 0, ..., X_{\frac{N}{2}-1}, 0, 0, 0, X^*_{\frac{N}{2}-2}, .., 0, X^*_{2}, 0\right] \tag{16}$$

$X_k$ represents the $k^{th}$ symbol modified using complex-valued QAM, with a mean of zero and a variance,

$$\sigma_X^2 = E\left[\left|X_k\right|^2\right]$$

The symbol E[·] represents the expectation operation. Subsequently, the time-domain DCO-OFDM signals may be acquired by the N-point IFFT operation, yielding the following results:

$$x_n = x(n) = \frac{1}{\sqrt{N}} \sum_{k=0}^{N-1} X_k e^{\frac{j2kn\pi}{N}}; 0 \le n \le N-1 \tag{18}$$

The transmitted signals of the DCO-OFDM branch are produced by removing the negative component of $x_n + B_{DC,DCO}$ by clipping,

$$x_{n,DCO} = \begin{cases} x_n + B_{DC,DCO};\ x_n + B_{DC,DCO} \ge 0 \\ 0;\ x_n + B_{DC,DCO} < 0 \end{cases} \tag{19}$$

The time-domain ACO-OFDM signals may be obtained after performing the N-point IFFT method,

$$Y = \left[0, Y_1, 0, Y_3, ..., Y_{\frac{N}{2}-1}, 0, Y^*_{\frac{N}{2}-1}, .., Y^*_{1}\right] \tag{20}$$

$$y_n = y(n) = \frac{1}{\sqrt{N}} \sum_{k=0}^{N-1} Y_k e^{\frac{j2kn\pi}{N}}; 0 \le n \le N-1 \tag{21}$$

In contrast to the DCO-OFDM branch, the unipolar ACO-OFDM signals are generated by removing the negative portion of $y_n$ by clipping.

$$y_{n,ACO} = \begin{cases} y_n;\ y_n \geq 0 \\ 0;\ y_n < 0 \end{cases} \tag{22}$$

The formulation of the transmitted ADO-OFDM signals may be achieved by combining ACO-OFDM signals with DCO-OFDM signals.

$$T_{n,ADO} = x_{n,DCO} + y_{n,ACO}; 0 \leq n \leq N-1 \tag{23}$$

The ADO-OFDM signal may be mathematically represented, taking into account the nonlinearity of the LED.

$$T_{n,ADO}^{Clipping} = \begin{cases} \delta_{upper}; T_{n,ADO} > \delta_{upper} \\ T_{n,ADO}; 0 \leq T_{n,ADO} \leq \delta_{upper} \\ 0; T_{n,ADO} < 0 \end{cases} \tag{24}$$

The symbol $\delta_{upper}$ represents the highest allowable voltage. At the receiver end, the optical signals that have been received are first transformed into electrical signals via the use of a photo detector. Next, the electrical signals that have been received undergo the procedure of eliminating the CP and performing the FFT operation [16]. The ACO-OFDM receiver may estimate the generated ACO-OFDM symbols on odd subcarriers. Subsequently, the ACO-OFDM signals in the time domain may be recreated and then subtracted from the received signals. After the interference cancellation technique, it is possible to estimate the DCO-OFDM symbols from even subcarriers.

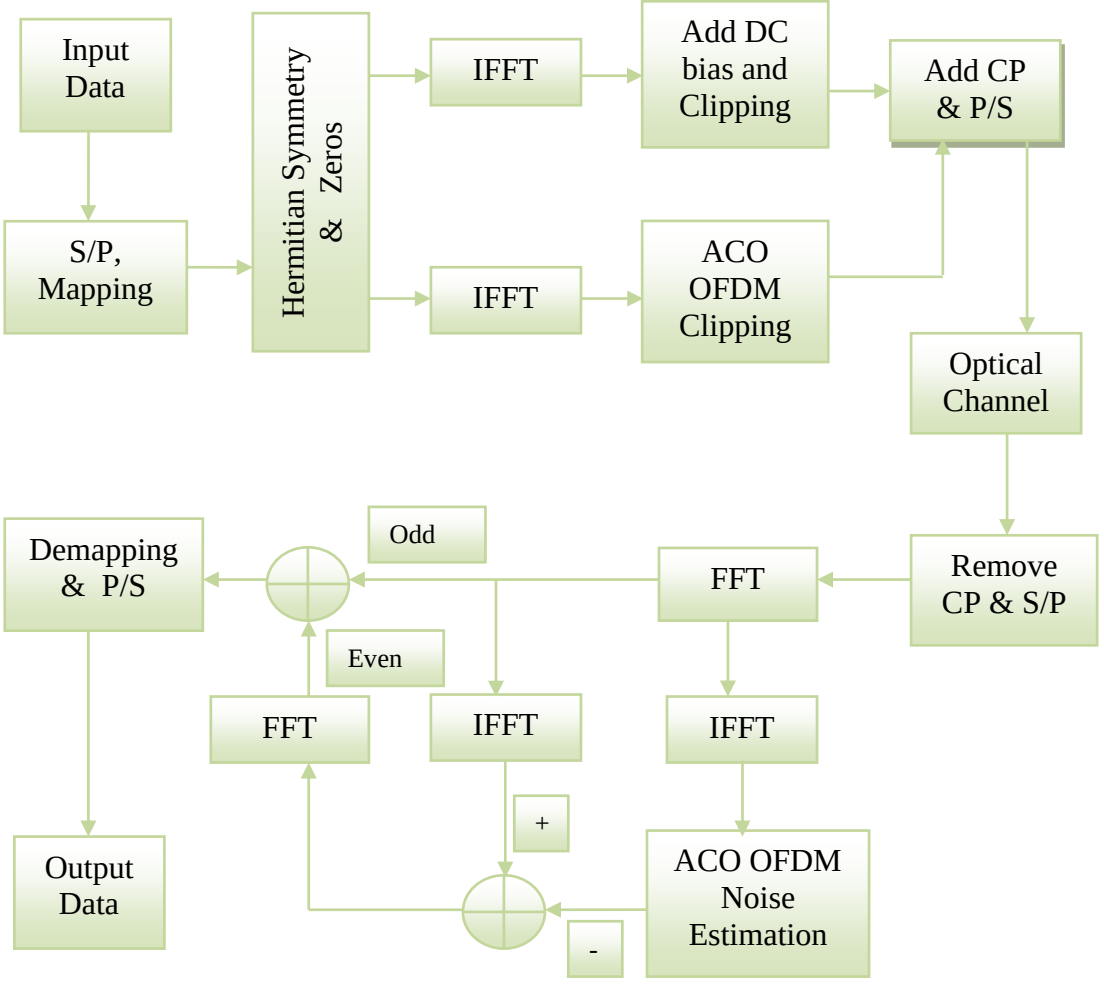


Fig.3. ADO-OFDM

### 2.5 LACO-OFDM

The technique known as LACO-OFDM uses the Fourier transform property and combines numerous layers of ACO-OFDM signals to enable simultaneous transmission. This approach demonstrated superior power and achieved enhanced spectrum efficiency in comparison to typical O-OFDM systems. In the a[th] LACO-OFDM layer, it was observed that only certain subcarriers, given by the formula $2^{a-1}(2m+1)-t; m=1,2,\ldots,\frac{N}{2^{a-1}}$ were modulated, while the other subcarriers were set to 0 [17]. The IFFT method provided a time-domain signal for the a[th] layer. The time-domain signal may be created by overlaying several ACO-OFDM signals, which can be defined as follows [18]:

$$X_{LACO,n}=\sum_{a=1}^{L}\left[X_{A,n}^{a}\right]_{c};n=0,1,..,N-1 \tag{25}$$

$$X_{A,n}^{a}=\frac{1}{\sqrt{N}}\sum_{i=0}^{N-1}X_{A,i}^{a}e^{\frac{j2\pi in}{N}} \tag{26}$$

$$X_{A,n}^{a}=\frac{1}{\sqrt{N}}\sum_{m=0}^{\frac{N}{2^{a}-1}}X_{A,2^{a}-1(2m+1)}^{a}e^{\frac{j2\pi(2m+1)n}{\frac{N}{2^{a}-1}}} \tag{27}$$

The symbols broadcast in the a[th] layer were free from interference and were successfully received by the receiver after performing the FFT procedures. Therefore, the disruption that occurred in Layer-1 may be restored using all the estimated symbols. After removing the regenerated interference from the received signals, an estimation of the broadcast symbol for the 2nd layer is obtained. Furthermore, the receiver may use the interference cancellation method to identify all sent symbols for the remaining concealed layers. In addition, the thermal and shot noise may be represented as AWGN ($W_n$), whereas the received signal $r_n$ is described as

$$r_n=h_n x_{LACO,n}+W_n;n=0,1\ldots,N-1 \tag{28}$$

The incoming signals are inputted into the FFT blocks, where the symbols in the frequency domain may be represented as

$$R_k=H_k x_{LACO,k}+W_k;k=0,1\ldots,N-1 \tag{29}$$

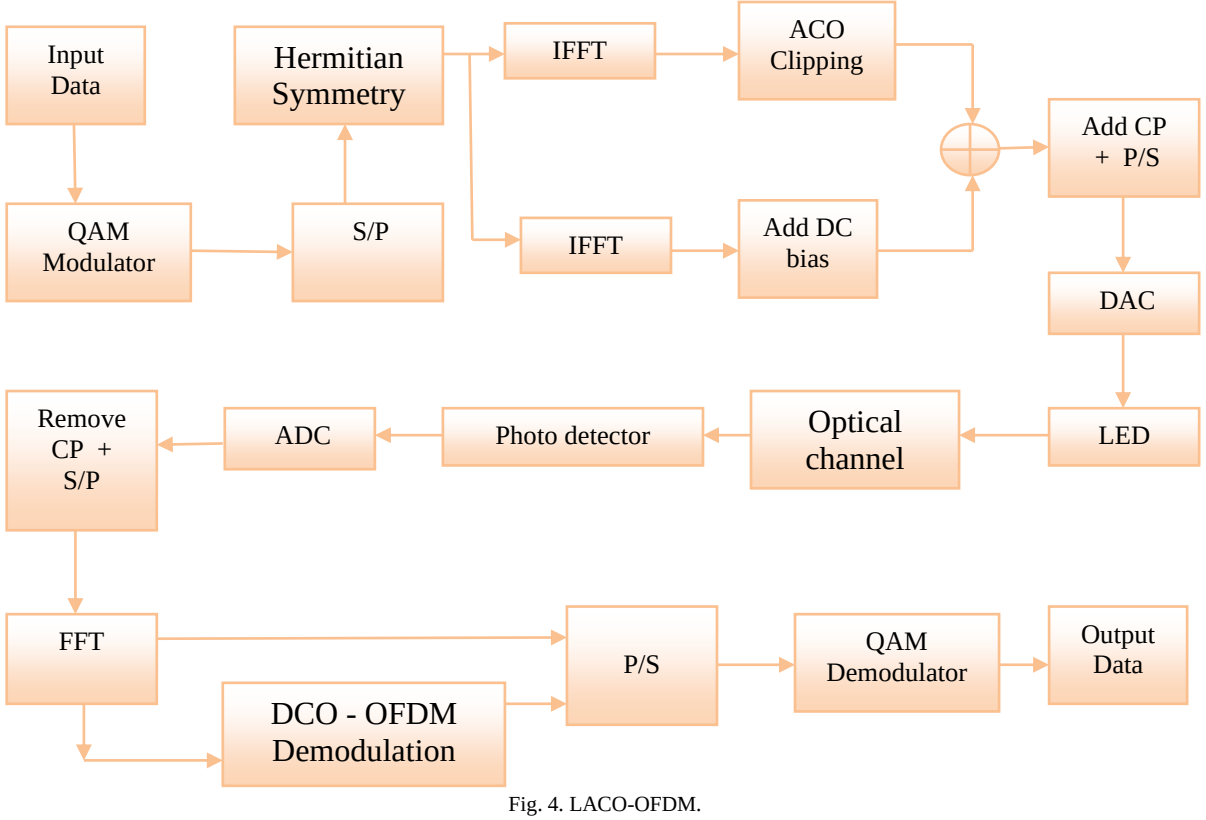


Fig. 4. LACO-OFDM.

## 3. PAPR

In OFDM, the amplitudes of the subcarriers exhibit variation, resulting in a large difference between the peak and average signal strength of the composite signal. OFDM methods that rely on IM/DD also experience the issue of PAPR. The PAPR issue is an undesirable occurrence that occurs as a result of the IFFT of data [19]. This results in the emission of radiation both inside and outside of the desired frequency range. Clipping is the most basic approach for managing PAPR, where the amplitudes of certain subcarriers are intentionally limited. This excerpt discusses the presence of both in-band and OoB interference, which disrupts the orthogonality between subcarriers. Subsequently, new coding procedures were created that include the selection of code words that minimize PAPR [19]. The approaches, such as PTS [20-21], tone reservation (TR) [22], and SLM [23], are devoid of distortion and interference. However, they need the use of side information.

### 3.1 Clipping

Clipping is a process where the signal is deliberately limited to decrease fluctuations in amplitude. If the amplitude of any subcarrier ($X_S$) exceeds a specified threshold ($\phi$), the signal is clipped.

$$X_s^{clipping} = \begin{cases} X_s; 0 \le X_s \le \phi \\ \phi; X_s > \phi \end{cases} \tag{30}$$

Consequently, when the signal is clipped, it is lost, and the total strength of the transmission is also diminished. Therefore, the use of the clipping approach causes distortion and results in a decrease of the BER [19]. Hence, it is advisable to perform clipping on a limited quantity of subcarriers.

### 3.2 SLM

SLM is designed to mitigate the effects of a high PAPR by selectively altering the transmitted signal. The method uses a set of carefully designed phase sequences called phase factors, which are then used on the initial symbols. Prior to transmission, the phase factors are generated and stored in a lookup table at both the transmitting and receiving ends. In the case of OFDM, a high signal peak value indicates a need for a significant DC bias, which results in significant deterioration of the system's power efficiency. Hence, this section presents an expanded Selected Mapping approach, which is a reduction strategy influenced by SLM. The SLM method is a widely used technique for reducing the PAPR [23]. It is straightforward to use and does not introduce any signal distortion. Additionally, it is compatible with any subcarrier number and modulation style [24]. In order to enhance the performance of PAPR reduction in the SLM scheme, it is necessary to augment the quantity of phase sequences used in the SLM approach. Nevertheless, the computing complexity of the SLM scheme exhibits a linear growth pattern in direct proportion to the number of phase sequences. An alternate approach involves doing a thorough search to find the most efficient sequence that results in the lowest PAPR. Therefore, in the SLM technique, the decrease of PAPR is mostly determined by the selected phase sequence candidates [25]. Our suggested strategy aims to train the network to decrease the PAPR while maintaining the BER performance. Therefore, it is necessary to consider two separate aspects simultaneously. According to the simulation, reducing the high PAPR and minimizing distortion can enhance the BER performance.

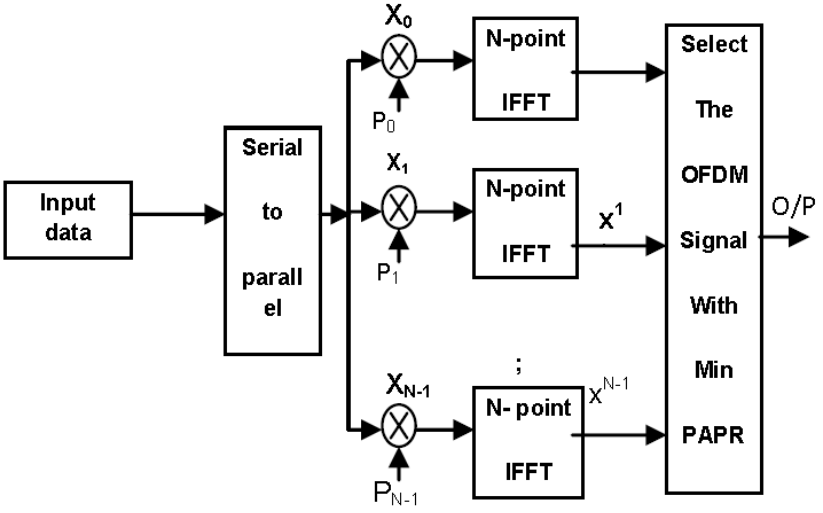


Fig. 5. SLM diagram

### 3.3 PTS

The PTS algorithm is a commonly used strategy for reducing PAPR in OFDM systems. It allows numerous users to share the same time-frequency resources by assigning varying power levels to each user's signal. Nevertheless, high PAPR values might still pose a potential issue in OFDM, resulting in signal distortion and a decline in performance. The PTS algorithm seeks to alleviate these difficulties by strategically modifying the broadcast signal [26]. Within the context of PTS, the initial OFDM signal is partitioned into many sub-blocks, and each sub-block is then fragmented into smaller partitions. The method does a thorough search of various combinations of phase factors for each division in order to identify the ideal phase sequence that minimizes the PAPR [20-21]. The PTS method tries to decrease the PAPR of the OFDM signal by doing a thorough search of the phase factors for each division. Nevertheless, this thorough investigation may be computationally demanding, particularly as the quantity of sub-blocks and divisions grows. Hence, it is necessary to take into account the trade-offs between the performance of reducing PAPR and the computational complexity in practical applications [27]. Figure 3 displays the block diagram of PTS.

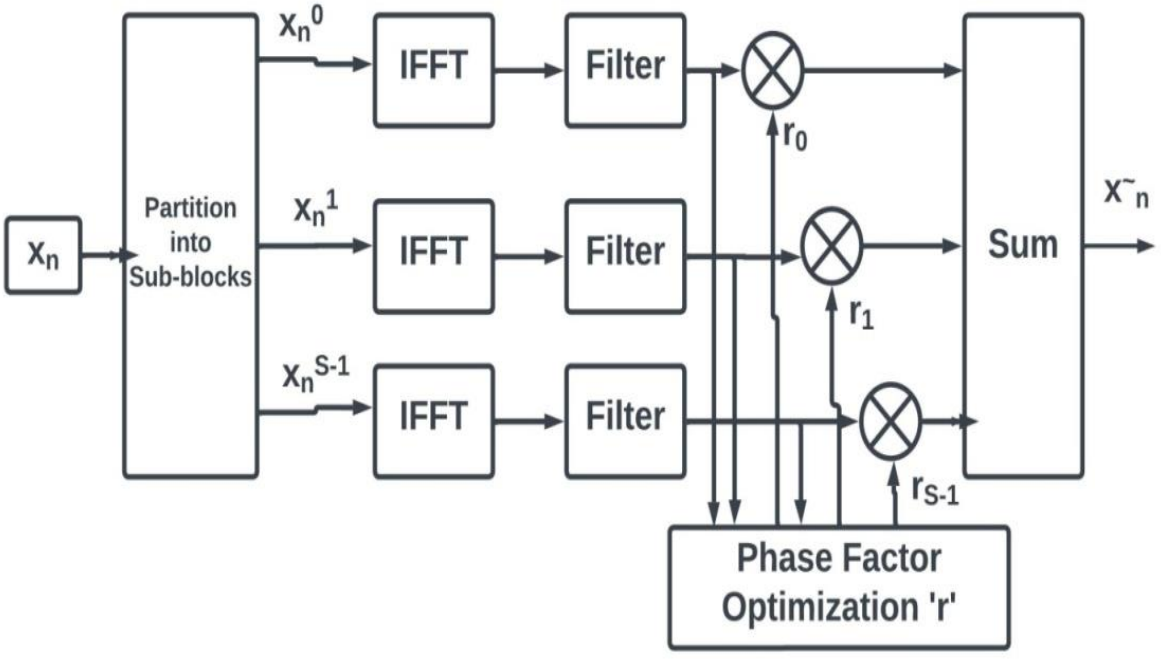


Fig. 6. PTS digram

## 4. SIMULATION RESULTS

This section presents an analysis of the performance of PAPR, BER, and Spectral Efficiency for the Clipping, SLM, and PTS methods in the LACO-OFDM structure. In addition, the LACO-OFDM is compared to the DCO-OFDM, ACO-OFDM, and ADO-OFDM. The primary objective of the essay is to decrease the PAPR of the OFDM system. The CCDF is a statistical metric that assesses the occurrence of signal peaks. On the other hand, PAPR measures the dynamic range of the signal. Both of these metrics are essential for assessing and improving the performance of waveforms.

The suggested and standard approaches are used to estimate the PAPR curves of the OFDM waveforms, as seen in the Figure 7. The SLM approach achieves superior decrease in PAPR. By partitioning the initial data stream into many smaller segments and assigning distinct phase factors to each segment, the maximum amplitudes are evenly spread among the various segments. The variation in the signal's amplitude helps to decrease the chances of many high peaks happening at the same time, resulting in a reduced overall PAPR of the transmitted signal. The LACO-OFDM approaches successfully reduced the PAPR by more than 1.5 dB for Clipping and 3.5 dB for SLM, with a probability of $10^{-2}$. The PAPR values for the DCO-Clipping, ACO-Clipping, DCO-LSM, ADO-Clipping, ACO-SLM, LACO-Clipping, ADO-SLM, and LACO-SLM methods are around 9.75dB, 8.1dB, 7.27dB, 6.76dB, 6.45dB, 6.41dB, 5.64dB, and 5.39dB, respectively, at a CCDF of $10^{-2}$.

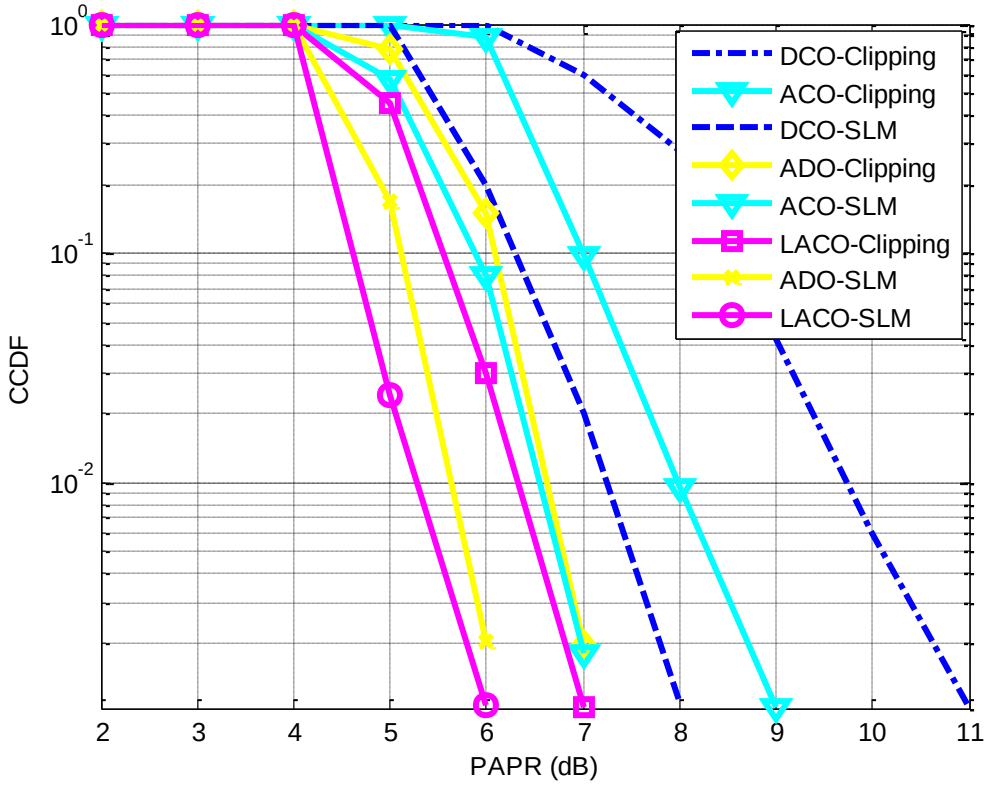


Fig. 7. PAPR for various OFDM schemes

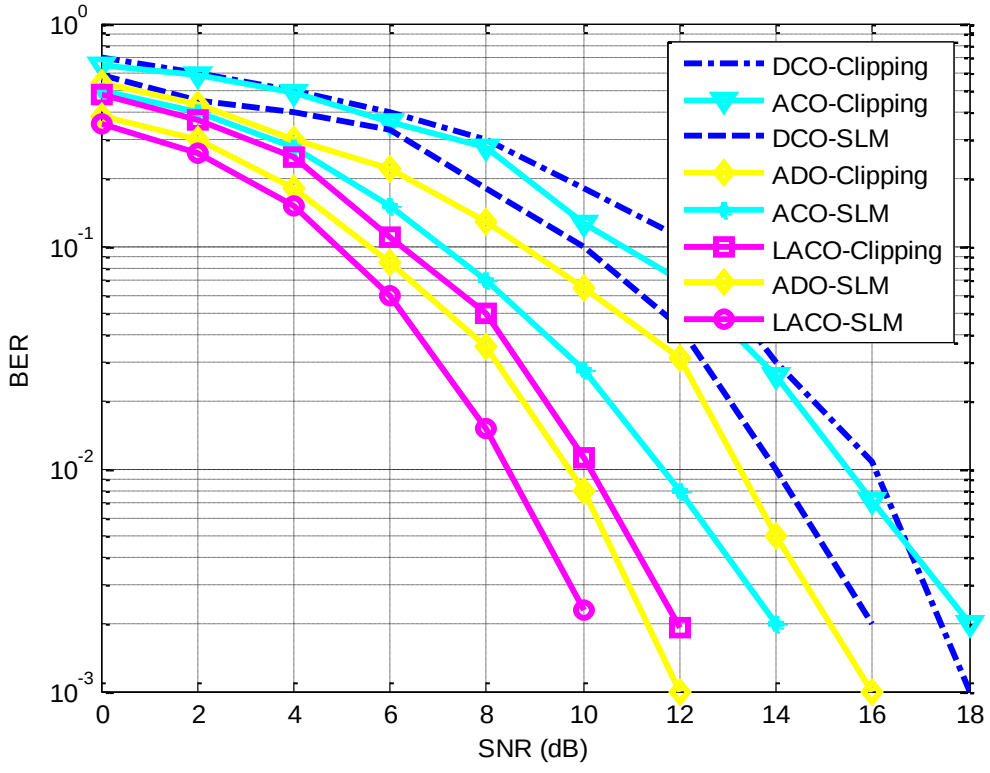


Fig. 8. BER vs SNR

The figure 8 displays the estimated BER performance of the OFDM signal using both clipping and SLM PAPR reduction techniques. The framework using the SLM approach exhibits superior performance in terms of BER compared to the clipping method. The BER performance exhibits marginal improvement when the SNR is raised from 0 to 18dB. The DCO-OFDM has the lowest performance when compared to the other approaches being considered. LACO-OFDM has greater performance in comparison to other methods. The SNR values for the methods DCO-Clipping, ACO-Clipping, DCO-SLM, ADO-Clipping, ACO-SLM, LACO-Clipping, ADO-SLM, and LACO-SLM with a BER CCDF of $10^{-2}$ are approximately 15.9dB, 15.69dB, 13.94 dB, 13.21 dB, 11.97 dB, 10.02 dB, 68B, and 8.19dB, respectively.

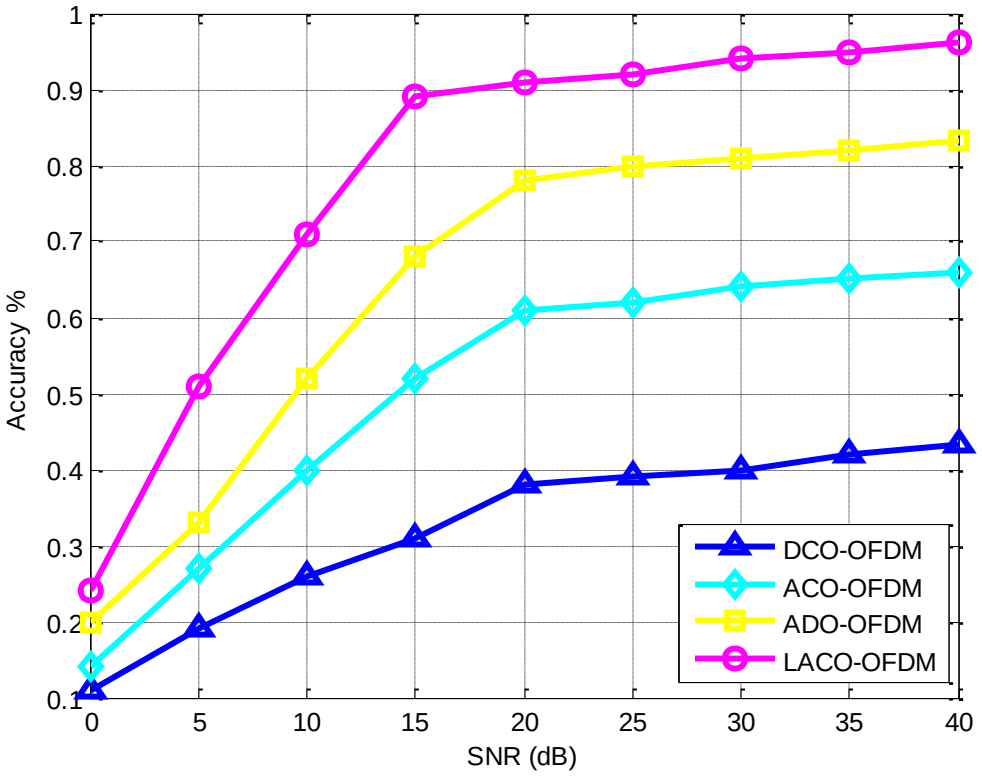


Fig. 9. SNR vs Accuracy

The figure 9 depicts the classification accuracy of the proposed LACO-based OFDM system in relation to other current approaches. The figure strongly illustrates the superiority of the proposed technique over the performance of the current existing methodologies. The LACO-OFDM system reaches a level of accuracy above 95% when the SNR is 40 dB.

## 5. CONCLUSION

Future wireless communication systems may use OFDM. OFDM requires orthogonality and subcarriers for information transfer. FFT is also fundamental to OFDM. FFT drastically alters subcarrier amplitude, causing PAPR. This study compares DCO, ACO, ADO, and LACO-OFDM performance. The PAPR, accuracy, and BER results are attained. Noise is only present on even subcarriers in ADO-OFDM, whereas information is conveyed on both even and odd subcarriers. Furthermore, in all of the methods, the enhancement in PAPR is achieved at the expense of signal power degradation and the introduction of extra distortion to the original signals. The effectiveness of the suggested SLM PAPR reduction approach in decreasing the PAPR in LACO-OFDM is exhibited in this research. The use of LACO-OFDM results in a substantial decrease in PAPR, which in turn enhances power efficiency and overall system performance. The BER examination shows a significant reduction in errors, suggesting improved signal reliability and quality. The findings demonstrate the ability of the SLM method to effectively reduce the PAPR in the LACO-OFDM system. This enables improved performance and spectral efficiency in 5G and future 5G waveforms.

## Conflicts Of Interest

No competing financial interests are reported in the author's paper.

## Funding

No grant or sponsorship is mentioned in the paper, suggesting that the author received no financial assistance.

## Acknowledgment

The author would like to thank the institution for creating an enabling environment that fostered the development of this research.

## References

[1] K. K. Vaigandla and B. J, "Study and analysis of multi carrier modulation techniques – FBMC and OFDM," Materials Today: Proceedings, vol. 58, pp. 52-56, 2022. DOI: 10.1016/j.matpr.2021.12.584.

[2] K. K. Vaigandla, M. Siluveru and S. R. Bolla, "Analysis of PAPR and Beamforming For 5G MIMO-OFDM," International Journal of Analytical and Experimental Modal Analysis, vol. XII, no. X, pp. 483-490, 2020.

[3] K. K. Vaigandla and J. Benita, "PRNGN - PAPR Reduction using Noise Validation and Genetic System on 5G Wireless Network," International Journal of Engineering Trends and Technology, vol. 70, no. 8, pp. 224-232, 2022. Crossref.

[4] J. Zhou and Y. Qiao, "Low-PAPR asymmetrically clipped optical OFDM for intensity - modulation/direct-detection systems," IEEE Photonics Journal, vol. 7, pp. 1-8, 2015.

[5] A. A. Abdulkafi, M. Y. Alias, and Y. S. Hussein, "Performance analysis of DCO-OFDM in VLC system," in 2015 IEEE 12th Malaysia International Conference on Communications (MICC), IEEE, 2015, pp. 163-168.

[6] J. Tan, Z. Wang, Q. Wang, and L. Dai, "Near-optimal low-complexity sequence detection for clipped DCO-OFDM," IEEE Photonics Technology Letters, vol. 28, pp. 233-236, 2015.

[7] J. Zhou, Z. Zhang, T. Zhang, M. Guo, X. Tang, Z. Wang, et al., "A combined PAPR-reduction technique for asymmetrically clipped optical OFDM system," Optics Communications, vol. 366, pp. 451-456, 2016.

[8] K. K. Vaigandla, A. S. Rao, and K. Srikanth, "Study of Modulation Schemes over a Multipath Fading Channels," International Journal for Modern Trends in Science and Technology, vol. 7, pp. 34-39, 2021. DOI: 10.46501/IJMTST0710005.

[9] I. Sohn, "New SLM scheme to reduce the PAPR of OFDM signals using a genetic algorithm," ICT Express, vol. 2, pp. 63-66, 2016.

[10] K. K. Vaigandla, R. K. Siddoju, M. K. Vanteru, M. Devsingh, D. Prasad, "PAPR, SPECTRAL EFFICIENCY, BER AND SNR ANALYSIS OF OFDM: A NOVEL PARTIAL TRANSMIT SEQUENCE-PARTICLE SWARM OPTIMIZATION TECHNIQUE," International Journal on AdHoc Networking Systems (IJANS), vol. 13, no. 4, pp. 21-35, Oct. 2023. DOI: 10.5121/ijans.2023.13402.

[11] K. K. Vaigandla, M. Siluveru, and R. Karne, "Study and Comparative Analysis of OFDM and UFMC Modulation Schemes," Journal of Electronics Computer Networking and Applied Mathematics (JECNAM), vol. 3, no. 2, pp. 41-50, 2023. DOI: 10.55529/jecnam.32.41.50.

[12] K. K. Vaigandla and J. Benita, "A Novel PAPR Reduction in Filter Bank Multi-Carrier (FBMC) with Offset Quadrature Amplitude Modulation (OQAM) Based VLC Systems," International Journal on Recent and Innovation Trends in Computing and Communication, vol. 11, no. 5, pp. 288-299, 2023. DOI: 10.17762/ijritcc.v11i5.6616.

[13] N. Sivapriya, M. K. Vanteru, K. K. Vaigandla, and G. Balakrishna, "Evaluation of PAPR PSD Spectral Efficiency BER and SNR Performance of Multi-Carrier Modulation Schemes for 5G and Beyond," SSRG International Journal of Electrical and Electronics Engineering, vol. 10, no. 11, pp. 100-114, 2023. Crossref DOI: 10.14445/23488379/IJEEE-V10I11P110.

[14] Vaigandla et al., "ANALYSIS OF PAPR BER AND CHANNEL ESTIMATION IN MULTI CARRIER MODULATION SYSTEMS USING NEURAL NETWORKS," Journal of Theoretical and Applied Information Technology, vol. 102, no. 5, pp. 1785-1795, Mar. 2024.

[15] K. K. Vaigandla and J. Benita, "Novel Algorithm for Nonlinear Distortion Reduction Based on Clipping and Compressive Sensing in OFDM/OQAM System," International Journal of Electrical and Electronics Research (IJEER), vol. 10, no. 3, pp. 620-626, 2022. DOI: 10.37391/IJEER.100334.

[16] K. K. Vaigandla, "Communication Technologies and Challenges on 6G Networks for the Internet: Internet of Things (IoT) Based Analysis," in 2022 2nd International Conference on Innovative Practices in Technology and Management (ICIPTM), 2022, pp. 27-31. DOI: 10.1109/ICIPTM54933.2022.9753990.

[17] Q. Wang, Z. Wang, X. Guo, and L. Dai, "Improved receiver design for layered ACO-OFDM in optical wireless communications," IEEE Photonics Technology Letters, vol. 28, pp. 319-322, 2015.
[18] T. Zhang, H. Ji, Z. Ghassemlooy, X. Tang, B. Lin, and S. Qiao, "Spectrum efficient triple-layer hybrid optical OFDM for IM/DD-Based optical wireless communications," IEEE Access, vol. 8, pp. 10352-10362, 2020.
[19] K. K. Vaigandla and J. Benita, "Study and Analysis of Various PAPR Minimization Methods," International Journal of Early Childhood Special Education (INT-JECS), vol. 14, no. 3, pp. 1731-1740, 2022.
[20] K. K. Vaigandla and J. Benita, "A Novel PTS-SIGWO Algorithm for Minimization of PAPR in FBMC/OQAM System," International Journal of Recent Engineering Science, vol. 10, no. 4, pp. 36-47, 2023. Crossref.
[21] K. K. Vaigandla and J. Benita, "PAPR REDUCTION OF FBMC-OQAM SIGNALS USING PHASE SEARCH PTS AND MODIFIED DISCRETE FOURIER TRANSFORM SPREADING," ARPN Journal of Engineering and Applied Sciences, vol. 18, no. 18, pp. 2127-2139, Sept. 2023.
[22] Y. Xiao, M. Chen, L. Fan, J. Tang, Y. Liu, and L. Chen, "PAPR reduction based on chaos combined with SLM technique in optical OFDM IM/DD system," Optical Fiber Technology, vol. 21, pp. 81-86, 2015.
[23] K. K. Vaigandla and J. Benita, "Selective Mapping Scheme Based on Modified Forest Optimization Algorithm for PAPR Reduction in FBMC System," Journal of Intelligent & Fuzzy Systems, vol. 45, no. 4, pp. 5367-5381, Oct. 2023. DOI: 10.3233/JIFS-222090.
[24] N. Ta¸spınar and M. Yıldırım, "A novel parallel artificial bee colony algorithm and its PAPR reduction performance using SLM scheme in OFDM and MIMO-OFDM systems," IEEE Communications Letters, vol. 19, pp. 1830-1833, 2015. [CrossRef]
[25] J.-G. Yuan, Q. Shen, J.-X. Wang, Y. Wang, J.-Z. Lin, and Y. Pang, "A novel improved SLM scheme of the PAPR reduction technology in CO-OFDM systems," Optoelectronics Letters, vol. 13, pp. 138-142, 2017. [CrossRef]
[26] R. Sayyari, J. Pourrostam, and H. Ahmadi, "A low complexity PTS-based PAPR reduction method for the downlink of OFDM-NOMA systems," in IEEE Wireless Communications and Networking Conference (WCNC), Austin, TX, USA, 2022, pp. 1719-1724. DOI: 10.1109/WCNC51071.2022.9771812.
[27] Y. I. Tek, E. B. Tuna, A. Savaşcıhabeş, and A. Ozen, "A new PAPR and BER enhancement technique based on lifting wavelet transform and selected mapping method for the next generation waveforms," AEU - International Journal of Electronics and Communications, vol. 138, Aug. 2021, 153871.